

## Zirconium Phosphates Partially Exchanged with Transition-metal Ions: Characterisation and Stereochemical Changes induced by Heat Treatment †

By Lucilla Alagna and Anthony A. G. Tomlinson,\* Istituto di Teoria e Struttura Elettronica dei Composti di Coordinazione del C.N.R., Area della Ricerca di Roma, C.P.10, Monterotondo Staz., 00016 Rome, Italy  
Carla Ferragina and Aldo La Ginestra, Istituto di Metodologie Avanzate Inorganiche del C.N.R., Area della Ricerca di Roma, C.P.10, Monterotondo Staz., 00016 Rome, Italy

The  $\alpha$  and  $\gamma$  forms of zirconium phosphate partially exchanged (between 20 and 90%) with  $\text{Co}^{2+}$ ,  $\text{Ni}^{2+}$ , or  $\text{Cu}^{2+}$  have been characterised, and changes in stereochemistry about the metal ion followed using mainly electronic reflectance spectroscopy. The stereochemistries found in the room-temperature forms are the same as for the 100%-exchanged  $\alpha$  form reported previously, *i.e.* octahedral. After heating these materials at 400 °C (*i.e.* when layer structures are still present), the stereochemistries about the metal ions are different from those in 100%-exchanged forms. Further heating, to 900 °C (destruction of layer structure), leads to further stereochemical changes. The other phases remaining in such materials thus influence the geometry of the cavity between the layers. Evidence is presented for the presence of five-co-ordinate geometries (both trigonal bipyramidal and square-based pyramidal) for  $\text{Co}^{2+}$ - and  $\text{Ni}^{2+}$ -containing materials.

INORGANIC ion exchangers with a non-rigid layer structure, such as those based on zirconium phosphate, readily take up transition-metal ions (t.m.i.) from aqueous solution.<sup>1</sup> We have previously shown that in fully exchanged  $\alpha$ -zirconium phosphate the t.m.i. change stereochemistry when the materials are heated.<sup>2</sup> This work has been extended to partially exchanged materials, which are of interest for various reasons, not the least of which is their potential as catalysts. By analogy with t.m.i.-loaded zeolites,<sup>3</sup> the unique properties of zirconium phosphate (good thermal stability, non-rigid layer structure having an interplanar distance which is readily modified by variable water content and the particular t.m.i. present)<sup>2</sup> makes it a candidate for use in catalysis. Indeed, copper- and silver-exchanged zirconium phosphates undergo redox processes similar to those found in zeolite analogues.<sup>4</sup>

The most spectacular catalytic process involving such materials reported to date is the one-step synthesis of methyl isobutyl ketone (condensation of two acetone molecules  $\rightarrow$  dehydration  $\rightarrow$  hydrogenation of double bond) using 0.5% w/w exchanged-reduced palladium-zirconium phosphate.<sup>5</sup> Since the material is acting as a polyfunctional catalyst, the reaction is probably quite complex and before mechanisms can be put forward the starting partially converted t.m.i. forms require characterisation.

This work was therefore carried out with the aim of (i) establishing the temperatures at which partially exchanged materials (both  $\alpha$  and  $\gamma$  forms of zirconium phosphate) undergo phase changes, (ii) monitoring changes in geometry about the t.m.i. on heating the materials, and (iii) investigating whether the other phases necessarily present influence the cavity available to the t.m.i.

### EXPERIMENTAL

The methods used to prepare the materials were essentially the same as reported previously for the fully exchanged  $\alpha$

forms of zirconium phosphate, *i.e.* contacting or prolonged elution.<sup>1,2</sup> Interest was confined to conversions ranging from 20 to 90%. The materials examined are listed in Figure 1. Metals were analysed using a Varian Techtron 120 atomic absorption flame spectrophotometer and the phosphate content was determined colorimetrically.<sup>6</sup>

The other phases remaining in the t.m.i.-converted materials depend on the method of preparation adopted. Starting from the  $\alpha$ -hydrogen-sodium phase (which exchanged most readily) and operating with t.m.i. nitrate solutions (*i.e.* at pH 3) only the exchange  $\text{M}^{2+}\text{-Na}^+$  occurs and the phases  $\overline{\text{H}\overline{\text{H}}}$  are present. Conversely, when exchange is performed by contacting acetate solutions (pH 4–4.5) the t.m.i. exchanges both  $\text{Na}^+$  and  $\text{H}^+$  in the ratio  $\text{Na}^+ : \text{H}^+ = 2 : 1$ .

In the case of the  $\gamma$  forms, the starting material used was  $\overline{\text{H}\overline{\text{H}}}\cdot 2\text{H}_2\text{O}$  and therefore the materials contained these two phases (*i.e.* exchanged + starting material).

Differential thermal analysis (d.t.a.) and thermogravimetric measurements were used to monitor dehydration processes. These went to completion at 450 °C for the  $\alpha$  forms and at *ca.* 420 °C for the  $\gamma$  forms. Condensation of the remaining acid to pyrophosphate occurs between 450 and 650 °C for  $\alpha$  forms and between 420 and 700 °C for  $\gamma$  forms. A Mettler TA 2000 °C simultaneous t.g.-d.s.c. (differential scanning calorimetric) thermal analyser was used. Samples for spectral measurements were heated in a conventional muffle furnace at temperatures somewhat higher than phase conversion for the same period of time (*ca.* 3 h) and the materials checked using X-ray powder methods. All spectra were recorded on freshly prepared samples; only materials heated at 400 °C tended to rehydrate, but then only slowly (days).

Physical measurements were carried out as described previously.<sup>2</sup>

### RESULTS AND DISCUSSION

*Thermal Behaviour and Identification of Phases.*— Since more than one phase is present in all the materials,

† Presented in part at the 12th Annual Meeting of the Associazione Italiana di Chimica Inorganica, Trieste, Italy, September 1979; Proceedings, p. 177.

the d.t.a. and t.g. curves are composite and vary with the degree of conversion, the operating conditions (*i.e.* the starting material used), and the nature and amount of t.m.i. employed.

For the  $\alpha$  forms the water content increases from one to four molecules of water as the degree of conversion increases, whereas for the  $\gamma$  forms the increase is from two to four  $\text{H}_2\text{O}$  molecules. At low conversion ratios the increase in water content in the  $\gamma$  forms is not high ( $2.5\text{H}_2\text{O}$  at *ca.* 50% conversion) and the X-ray powder patterns of the materials obtained are very similar to that of  $\gamma\text{-Zr}(\text{HPO}_4)_2 \cdot 2\text{H}_2\text{O}$ .<sup>7</sup> It appears that significant structural changes begin to occur only after relatively high degrees of conversion have been reached.

The water content in the materials was calculated from

the weight losses at 450 °C ( $\alpha$  forms) and 400–420 °C ( $\gamma$  forms). As shown by the d.t.a. or d.s.c. curves, several endothermic reactions occur below 350–450 °C. This is a reflection of the fact that more than one phase is present (*i.e.*  $\alpha\text{-HH} \cdot \text{H}_2\text{O}$ ,  $\gamma\text{-HH} \cdot 2\text{H}_2\text{O}$ ,  $\text{NaH} \cdot 5\text{H}_2\text{O}$ , together with the 50% and 80%-exchanged t.m.i. forms); the results may be compared with the known dehydration curves for the former pure materials.<sup>8</sup> Above 420 °C ( $\gamma$ ) and 450 °C ( $\alpha$ ), condensation of the anhydrous HH phases present begins and, after the weight loss involved is complete, exothermic processes involving the t.m.i.-converted phases (*i.e.* anhydrous layer structure  $\rightarrow$  non-layer phases) occur (see Figure 1).

Turning to the  $\gamma$  forms, only after the exothermic transition (occurring in the range 600–850 °C) did the

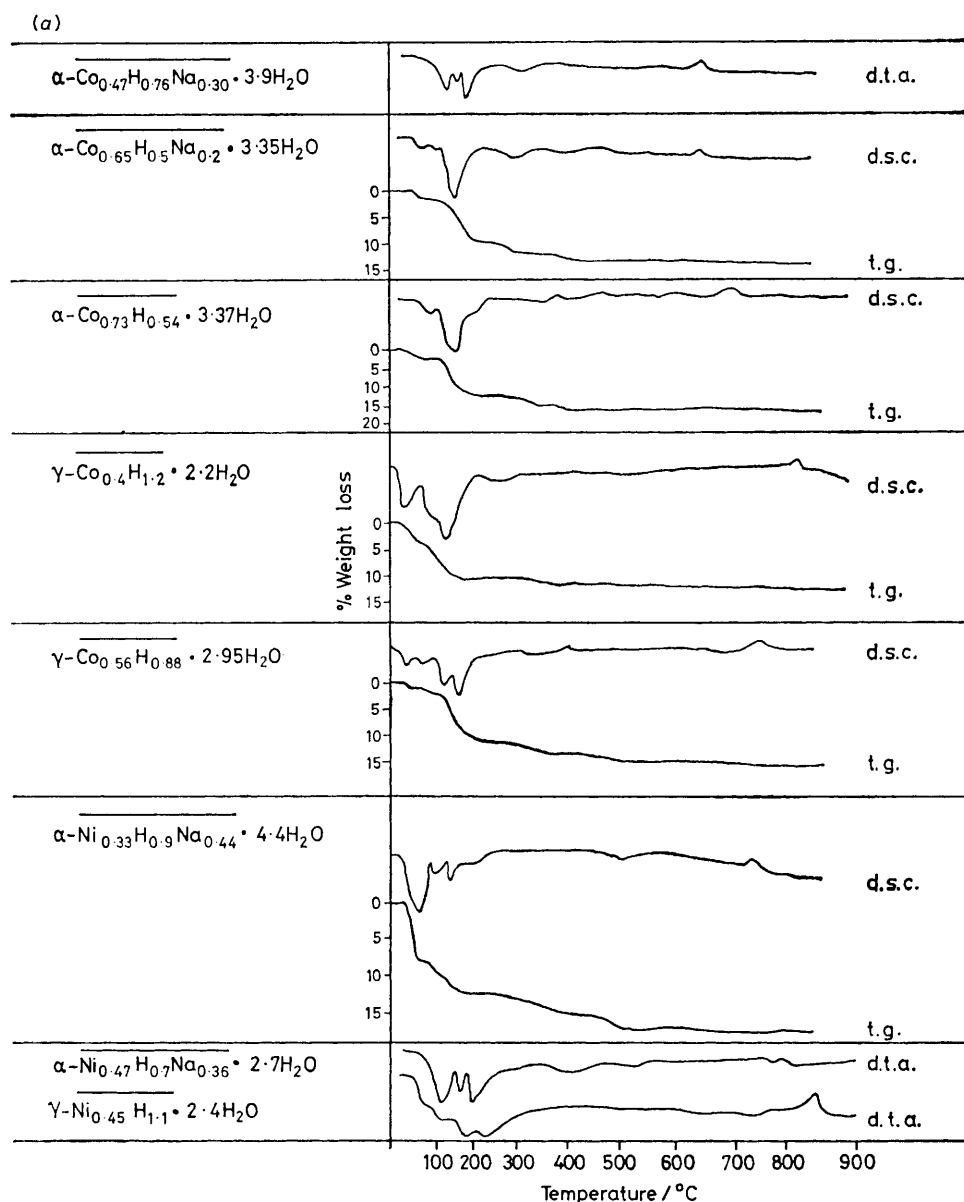
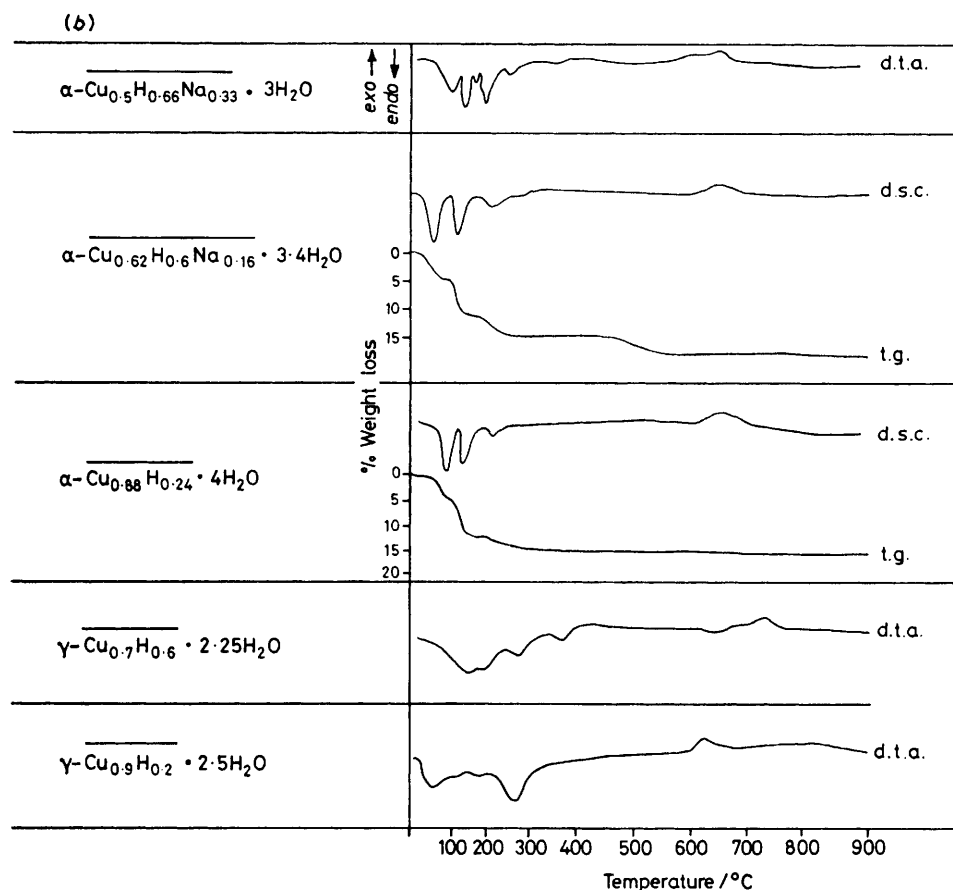


FIGURE 1 D.t.a., d.s.c., and t.g. curves of (a)  $\text{Co}^{2+}$ - and  $\text{Ni}^{2+}$ -exchanged  $\alpha$ - and  $\gamma$ -zirconium phosphate; (b)  $\text{Cu}^{2+}$ -exchanged  $\alpha$ - and  $\gamma$ -zirconium phosphate. Phases are indicated by a Greek letter, followed by the symbol of the exchanger, their counter ions, and any water molecules which may be present



materials obtained give X-ray powder patterns similar to those obtained from materials derived from the  $\alpha$  forms. Up to 650–700 °C the powder patterns of the phases obtained are very similar to those of the  $\gamma\text{-}\overline{\text{H}}\overline{\text{H}}$  phase calcined at 350 °C. We conclude that in the  $\gamma$  forms the phase transitions from layered to non-layered structures often require higher temperatures than is the case for the  $\alpha$  forms, before going to completion.

The X-ray patterns indicate that at 400–600 °C the  $\alpha$  forms all have  $d_{002}$  ca. 7 Å (6.8–7.4 Å) whereas all the  $\gamma$  forms have the same  $d_{002}$  as observed for  $\gamma\text{-}\overline{\text{H}}\overline{\text{H}}$  (*i.e.* 9.2 Å) (see Figure 2). The other peaks observed at 7.4 and 6.8 Å in the  $\gamma$  forms are presumably due to the t.m.i.  $\gamma$  phases.

At 900 °C, both  $\alpha$  and  $\gamma$  forms gave the expected double-phosphate type phases,  $\text{MZr}(\text{PO}_4)_2$ , although they are not exactly the same (Figure 3). In addition, these materials also contain phases derived from the starting materials, *i.e.*  $\text{ZrP}_2\text{O}_7$  [from  $\text{Zr}(\text{HPO}_4)_2 \cdot n\text{H}_2\text{O}$ ] or  $\text{NaZr}_2(\text{PO}_4)_3$  (from  $\text{NaH} \cdot 5\text{H}_2\text{O}$ ).

**Metal-ion Stereochemistries.—Room-temperature phases.** As for the fully exchanged  $\alpha$  forms, all the partially exchanged materials have  $\text{Co}^{2+}$  and  $\text{Ni}^{2+}$  in octahedral environments and the  $\text{Cu}^{2+}$  in a tetragonally distorted co-ordination in the hydrated phases.<sup>2</sup> The presence of the other phases thus appears to influence the t.m.i. environment available in the cavity very little (see

Tables 1–3). However, although the gross stereochemistry is the same for both  $\alpha$  and  $\gamma$  forms, there are very small, but systematic, differences between the two forms. Thus, in the  $\gamma$  forms there are slight shifts to lower energy compared with corresponding bands in the  $\alpha$  analogues, *e.g.*  $\nu_3$  for  $\text{Ni}^{2+}$  ( $\gamma$ ) phases lies at 8 300  $\text{cm}^{-1}$ , whilst for  $\text{Ni}$  ( $\alpha$ ) phases it is found at 8 700  $\text{cm}^{-1}$ . A similar, although less marked, effect is found in the  $\text{Co}^{2+}$ - and  $\text{Cu}^{2+}$ -exchanged phases. As  $\text{PO}_4^{3-} < \text{H}_2\text{O}$  in the spectrochemical series,<sup>9</sup> this implies that in the  $\gamma$  forms the t.m.i. is co-ordinated to more oxygen atoms from  $\text{PO}_4^{3-}$  groups (rather than from water molecules) than is the case for the  $\alpha$  forms. The different inter-planar distances and, possibly, different orientations of the phosphate oxygen atoms are already sufficient to lead to small differences in environment about the t.m.i. in the cavity (see refs. 10 and 11 for structural differences believed to exist between the two forms). In a similar vein, partially dehydrated forms in which the t.m.i. is still octahedral show band shifts indicative of oxygen environments arising from  $\text{PO}_4^{3-}$  rather than from  $\text{H}_2\text{O}$  and this is again more evident in the  $\text{Ni}^{2+}$ -loaded materials (Table 2).

**Cobalt(II)- and nickel(II)-loaded anhydrous layer phases.** After complete dehydration, the layer structures remaining have t.m.i. in stereochemistries different to those in the hydrated forms. For example,  $\text{Co}^{2+}$

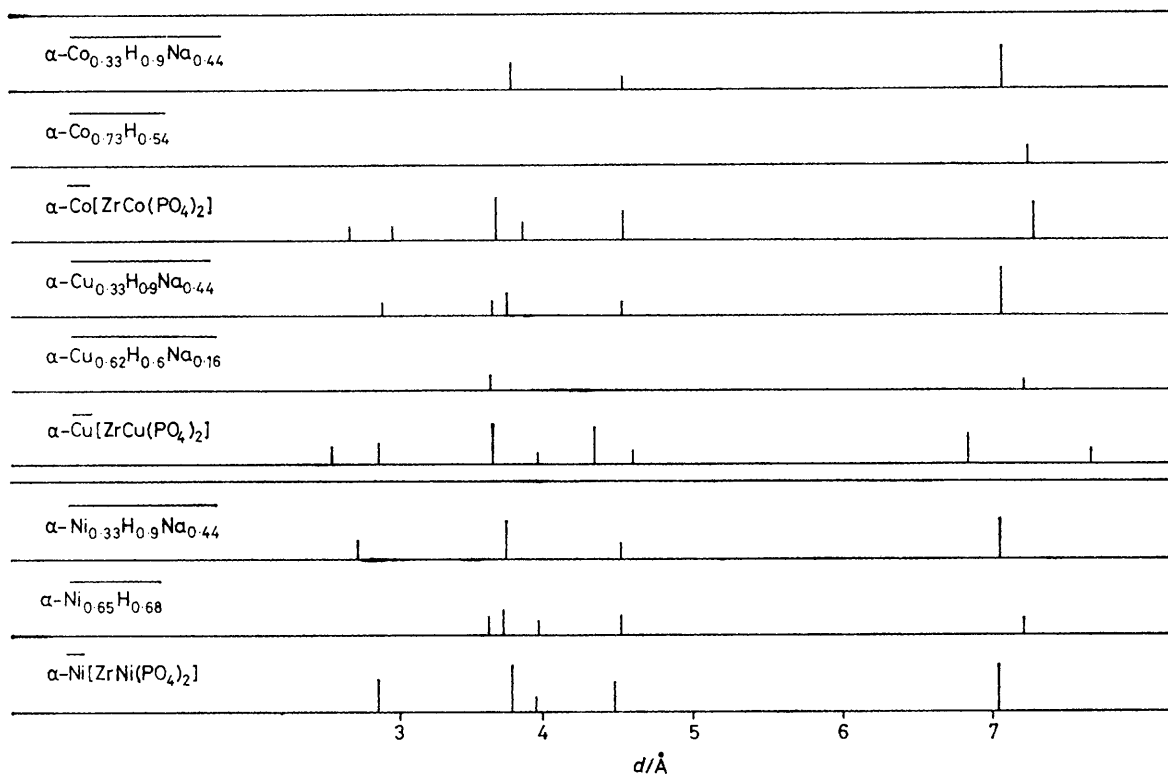


FIGURE 2 X-Ray powder patterns of the materials after heating at 400 °C

passes from an octahedral to a tetrahedral stereochemistry in both  $\alpha$  and  $\gamma$  forms (see Figure 4). However, there are differences between the two:  $Dq(\gamma) = 470 \pm 10 \text{ cm}^{-1}$  and  $Dq(\alpha) = 420 \pm 10 \text{ cm}^{-1}$  (using König's method;<sup>12</sup> uncertainties are due to difficulty in locating the exact midpoint of the  ${}^4T_1(F) \leftarrow {}^4A_2$  transition in the near i.r.). Apart from slight changes in the energies of the components of the  ${}^4T_1(P) \leftarrow {}^4A_2$  transition in the visible region, there is little difference between the reflectance spectra of highly loaded materials and those with lower  $\text{Co}^{2+}$  loadings (see Table 1).

The situation is more complicated in layer-structure phases containing  $\text{Ni}^{2+}$ . The environment(s) now available to the metal ion appear to depend on both factors, *i.e.* change in interplanar spacing between  $\alpha$  and  $\gamma$  forms and degree of loading.  $\alpha$  Forms which are  $\geq 50\%$  exchanged gave reflectance spectra which are variants of that assigned to a tetrahedral stereochemistry for the fully exchanged  $\alpha$  form.<sup>2</sup> It is well known that even slight changes in angular distortion can lead to rather large changes in electronic spectra for this stereochemistry.<sup>13</sup> However, the spectral changes found in materials having low  $\text{Ni}^{2+}$  loadings are too large for them to be considered 'distorted tetrahedral'. Thus,  $\alpha\text{-Ni}_{0.33}\text{H}_{0.9}\text{Na}_{0.44}$  (from acetate) gives a spectrum with bands at 9 800, 15 900, and 21 750  $\text{cm}^{-1}$ , clearly distinguishable from those of octahedral and tetrahedral geometries. In addition, the magnetic moment of  $3.4 \pm 0.05 \text{ B.M.}^*$  (somewhat lower than that, 3.69 B.M., of the

\* Throughout this paper: 1 B.M. =  $9.274 \times 10^{-24} \text{ A m}^2$ .

$100\%$ -exchanged  $\alpha\text{-Ni}^{2+}$ ) excludes the presence of 'mixed' co-ordinations involving a diamagnetic  $\text{Ni}^{2+}$  ion, *e.g.* square planar + octahedral.<sup>14</sup> The implication is that a five-co-ordinate stereochemistry is present and although a trigonal-bipyramidal (t.b.p.)  $\text{NiO}_5$  is not available in the literature, the number, energies, and intensities of the bands are all very close to those expected for this geometry.<sup>15</sup> Although we can say little about the exact distortions present, these differences between materials of low loading provide a nice demonstration of near-neighbour interaction with ions remaining within the lattice. The only difference between these 33%-exchanged  $\alpha$  forms after heating at 400 °C is that one (from acetate solution) contains more  $\text{NaH}$  phase than the other (from nitrate solution). However, they adopt different stereochemistries, the former five-co-ordinate, the latter tetrahedral (Figure 5).

The  $\text{Ni}^{2+}$ -exchanged  $\gamma$  forms adopt a different stereochemistry from the  $\alpha$  forms, but the degree of loading appears to have less influence. The spectrum again points to a five-co-ordinate environment, the band shape being strikingly similar to that of  $[\text{Ni}(\text{dacoda})(\text{OH}_2)]$  (dacoda = 1,5-diazacyclo-octane-*NN'*-diacetate) of known square-pyramidal (s.p.) geometry.<sup>16</sup> It also compares well with the spectrum of  $[\text{Ni}(\text{AsMePh}_2\text{O})_4(\text{NO}_3)][\text{NO}_3]$ , also s.p. and with five unidentate oxygen-containing ligands probably of similar strength as the phosphate groups dealt with here.<sup>17</sup> This model complex has major triplet-triplet bands at 8 200 [ ${}^3A_2(F)$ ], 9 300 [ ${}^3B_2(F)$ ], 11 900 [ ${}^3E(F)$ ], 19 000 [ ${}^3A_2(P)$ ], and

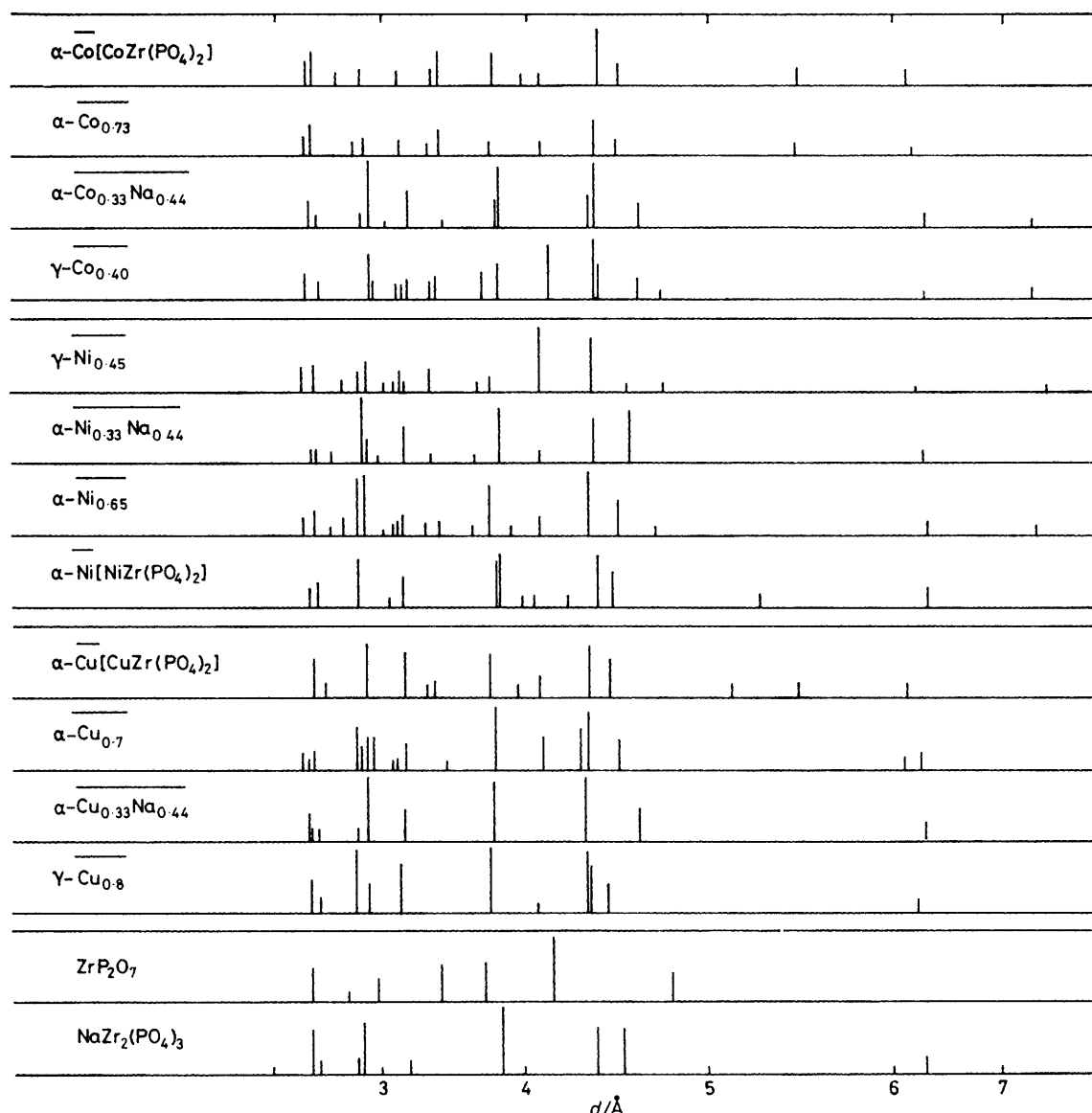


FIGURE 3 X-Ray powder patterns of the materials after heating at 900 °C

22 900  $\text{cm}^{-1}$  [ ${}^3E(P)$ ] ( ${}^3B_1$  ground state). The comparison is reasonable (energies to  $\pm 1000 \text{ cm}^{-1}$ , relative intensities as expected for *ca.*  $C_{4v}$  geometry), splitting of the most intense band in the visible region presumably indicating that some distortion (angles or bond lengths) is present.

*Cobalt(II)- and nickel(II)-loaded non-layer structures.* Given that destruction of the layer structure by heating at 900–950 °C gives materials with a very similar phase starting from  $\text{Co}^{2+}$ -exchanged  $\alpha$  or  $\gamma$  forms, it would be expected that the stereochemistry available to the metal ion would be the same in both cases. Nevertheless, the degree of loading exerts some influence. Thus, in the  $\gamma$  forms, loadings above and below 50% gave the same spectra (see Figure 6) which are also the same as found for the non-layered 100%-exchanged material.<sup>2</sup> We previously suggested that such very large splittings in

the near-i.r. region was due to the presence of very large distortions in a tetrahedral geometry (the splittings are much larger than in oxide-based analogues, such as  $\text{CoO-ZnO}$ <sup>18</sup>). In the interim, evidence has accumulated to show that a two-component band [derived from the t.b.p.  $b^4E(F)$  level split by a  $C_{2v}$  component] followed by another band (or two bands) much further into the near-i.r. region than expected for the  ${}^4T_1(F) \leftarrow {}^4A_2$  transition of  $T_d$  symmetry is diagnostic of a (close to) t.b.p. geometry.<sup>19</sup> The only slightly greater splitting in this band observed here ( $1600 \text{ cm}^{-1}$ ) compared with that in the almost regular t.b.p. model complex  $[\text{Co}(\text{ONC}_5\text{H}_4\text{-Me})_5][\text{ClO}_4]_2$  ( $1300 \text{ cm}^{-1}$ )<sup>20</sup> indicates that the geometry probably deviates only slightly from a regular t.b.p.

Cobalt(II)  $\alpha$  forms above 50% loading again give a t.b.p. geometry (see Figure 6). However, below 50% loading the spectra change considerably: only three

TABLE 1  
Cobalt(II)-containing materials

Heat treatment (°C)	Material	Colour	<i>d-d</i> Bands (cm <sup>-1</sup> )
ca. 25	$\alpha\text{-Co}_{0.47}\text{H}_{0.76}\text{Na}_{0.30}\cdot 3.9\text{H}_2\text{O}$	Pink	8 620br, 20 000s, 21 740 (sh)
	$\alpha\text{-Co}_{0.73}\text{H}_{0.54}\cdot 3.37\text{H}_2\text{O}$		
400	$\gamma\text{-Co}_{0.4}\text{H}_{1.2}\cdot 2.2\text{H}_2\text{O}$	Pink	8 000br, 19 380s, 21 370 (sh)
	$\gamma\text{-Co}_{0.56}\text{H}_{0.88}\cdot 2.95\text{H}_2\text{O}$		
	$\alpha\text{-Co}_{0.33}\text{H}_{0.9}\text{Na}_{0.44}$	Purple	7 140br, 15 870 (sh), 17 180s, 19 420 (sh), 20 000s, 21 050 (sh)
	$\alpha\text{-Co}_{0.73}\text{H}_{0.54}$	Purple	7 250br, 15 870 (sh), 17 180s, 19 050s, 19 230 (sh)
900	$\gamma\text{-Co}_{0.4}$	Purple	8 000br, 16 180s, 17 480s, 19 160s, 20 000 (sh)
	$\gamma\text{-Co}_{0.56}$	Pale blue	ca. 3 850vw, 6 060m, 8 130m, 12 050m, 17 540s, 19 420m, 21 500m
	$\alpha\text{-Co}_{0.33}\text{Na}_{0.44}$	Pale blue	4 780w, 5 930m, 9 220, 11 300m, 17 450s, 20 200 (sh), 20 830s, ca. 21 740 (sh)
	$\alpha\text{-Co}_{0.47}\text{Na}_{0.3}$	Violet	4 780w, 5 880m, 9 300m, 11 100m, 15 150 (sh), 17 540 (sh), 20 000 (sh), 20 830 (sh), 24 390vw
	$\alpha\text{-Co}_{0.73}$	Violet	4 800m, 5 900m, 9 300m, 11 170m, 15 380 (sh), 17 640s, 20 200 (sh)
	$\gamma\text{-Co}_{0.4}$ $\gamma\text{-Co}_{0.56}$	Violet	4 800m, 5 880m, 9 260m, 11 000m, 15 380 (sh), 17 390 (sh), 20 000 (sh), 20 410 (sh)

TABLE 2  
Nickel(II)-containing materials

Heat treatment (°C)	Material	Colour	<i>d-d</i> Bands (cm <sup>-1</sup> )
ca. 25	$\alpha\text{-Ni}_{0.33}\text{H}_{0.9}\text{Na}_{0.44}\cdot 4.4\text{H}_2\text{O}$	Pale green	8 770m,br, 15 625m, 26 040s
	$\alpha\text{-Ni}_{0.68}\text{H}_{0.68}$		
	$\gamma\text{-Ni}_{0.2}$		
400	$\gamma\text{-Ni}_{0.45}\text{H}_{1.1}\cdot 2.4\text{H}_2\text{O}$	Pale green	8 420br, 13 660m, 15 240 (sh), 20 320s, 26 600 (sh)
	$\alpha\text{-Ni}_{0.33}\text{H}_{0.9}\text{Na}_{0.44}$	Pale green	9 800w, 13 700vw, 15 870m, 21 740s
	$\alpha\text{-Ni}_{0.33}\text{HNa}_{0.34}$	Tan	5 780w, 11 240m, 16 670m, 19 230 (sh), 21 980s, 23 000 (sh)
	$\alpha\text{-Ni}_{0.68}\text{H}_{0.68}$	Tan	5 550w, 6 900w (sh), 11 700m, 16 950m, ca. 20 000 (sh), 23 530vs
	$\alpha\text{-Ni}_{0.8}$	Tan	4 400vw, 5 800vw, 7 100w, 16 300m, 21 700s, 23 500vs
	$\gamma\text{-Ni}_{0.2}\text{H}_{1.6}$	Pink	7 170m, 10 000s, 13 510vw (sh), 16 950m, 19 000s, 20 000s, 21 500s
	$\gamma\text{-Ni}_{0.45}\text{H}_{1.1}$	Pink	7 140m, ca. 7 690 (sh), 10 150s, 13 510vw (sh), 16 670 (sh), 18 870s, 20 000s, 21 280s
	900	$\alpha\text{-Ni}_{0.33}\text{Na}_{0.44}$	Yellow
$\alpha\text{-Ni}_{0.33}\text{Na}_{0.34}$		Yellow	5 900m, 7 400 (sh), 12 270m, 20 410 (sh), 23 700s
$\alpha\text{-Ni}_{0.68}$		Ochre	6 060w (sh), 7 690m, 12 350s, 16 800 (sh), 18 690 (sh), 20 530s, 23 420vs
$\alpha\text{-Ni}_{0.8}$			4 700w (sh), 5 500br, 12 200m, ca. 16 800 (sh), 20 530 (sh), 23 420s
$\gamma\text{-Ni}_{0.2}$		Pink	5 880w, 7 400 (sh), 10 500 (sh), 12 500s, 16 950 (sh), 18 520 (sh),
$\gamma\text{-Ni}_{0.45}$		Pink	20 400s, 23 640s

TABLE 3  
Copper(II)-containing materials

Heat treatment (°C)	Material	Colour	<i>d-d</i> Bands (cm <sup>-1</sup> )	
ca. 25	$\alpha\text{-Cu}_{0.33}\text{Na}_{0.44}\cdot 3\text{H}_2\text{O}$	Pale blue	13 400br	
	$\alpha\text{-Cu}_{0.6}\text{H}_{0.66}\text{Na}_{0.33}\cdot 3\text{H}_2\text{O}$	Pale blue	13 500br	
	$\alpha\text{-Cu}_{0.88}\text{H}_{0.24}\cdot 4\text{H}_2\text{O}$	Pale blue	13 300br	
	$\gamma\text{-Cu}_{0.24}\text{H}_{1.52}\cdot 2.1\text{H}_2\text{O}$	Pale blue	12 500vbr	
	$\gamma\text{-Cu}_{0.64}\text{H}_{0.72}\cdot 2.25\text{H}_2\text{O}$	Pale blue	12 600vbr	
	$\gamma\text{-Cu}_{0.7}\text{H}_{0.6}\cdot 2.25\text{H}_2\text{O}$	Pale blue	12 200vbr	
	$\gamma\text{-Cu}_{0.9}\text{H}_{0.2}\cdot 2.5\text{H}_2\text{O}$	Pale blue	11 900vbr	
	400	$\alpha\text{-Cu}_{0.33}\text{H}_{0.9}\text{Na}_{0.44}$	Pale blue	12 500vbr
		$\alpha\text{-Cu}_{0.6}\text{H}_{0.66}\text{Na}_{0.33}$	Pale blue	12 800vbr
		$\alpha\text{-Cu}_{0.88}\text{H}_{0.24}\cdot 2.5\text{H}_2\text{O}$	Pale blue	13 600vbr
		$\gamma\text{-Cu}_{0.24}\text{H}_{1.52}$	Inhomogeneous	11 100vbr
		$\gamma\text{-Cu}_{0.64}\text{H}_{0.72}$	Green	8 000 (sh) br, 11 100s,br
$\gamma\text{-Cu}_{0.70}\text{H}_{0.6}$		Turquoise	8 150s,br, 10 500 (sh)	
900	$\gamma\text{-Cu}_{1.0}$	Turquoise	ca. 7 700 (sh), 10 500s,br	
	$\alpha\text{-Cu}_{0.16}$	Pale green	11 800br, ca. 15 900 (sh)	
	$\alpha\text{-Cu}_{0.33}\text{Na}_{0.44}$	Pale green	9 200 (sh), 11 500br	
	$\alpha\text{-Cu}_{0.7}$	Pale green	11 200br, 15 400 (sh)	
	$\gamma\text{-Cu}_{0.8}$ ; $\gamma\text{-Cu}_{0.64}$	Pale blue	ca. 10 000 (sh), 11 700	

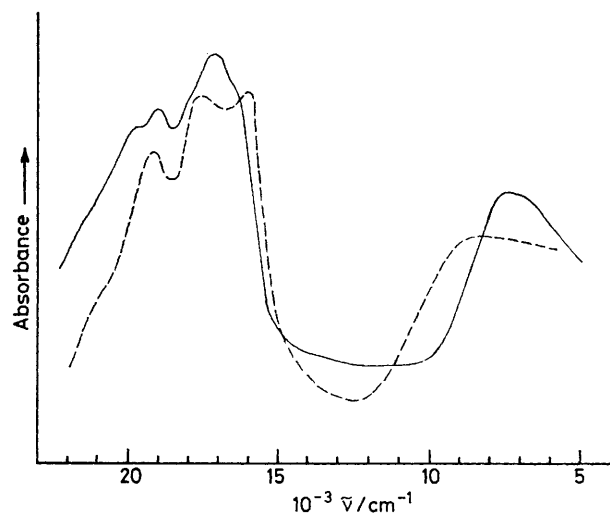


FIGURE 4 Electronic reflectance spectra of  $\text{Co}^{2+}$ -exchanged materials after heating at  $400^\circ\text{C}$ : (—),  $\alpha\text{-Co}_{0.73}\text{H}_{0.54}$ ; (---),  $\gamma\text{-Co}_{0.4}$

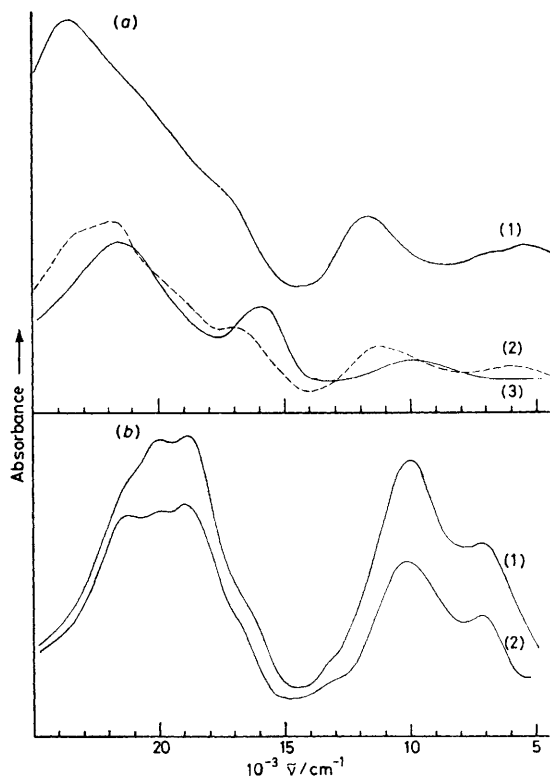


FIGURE 5 Electronic reflectance spectra of  $\text{Ni}^{2+}$ -exchanged materials after heating at  $400^\circ\text{C}$ . (a)  $\alpha$  Forms:  $\text{Ni}_{0.66}\text{H}_{0.68}$  (1);  $\text{Ni}_{0.33}\text{HN}_{0.34}$  (2);  $\text{Ni}_{0.33}\text{H}_{0.9}\text{Na}_{0.44}$  (3). (b)  $\gamma$  Forms:  $\text{Ni}_{0.45}\text{H}_{1.6}$  (1);  $\text{Ni}_{0.2}\text{H}_{1.6}$  (2)

bands are now present in the near-i.r. region, the shoulder at  $ca. 15\,400\text{ cm}^{-1}$  is no longer present, and the band shape is changed in the visible region. The band shapes and energies are very similar to those in  $[\text{Co}(\text{dacoda})(\text{OH}_2)]$  of (almost) s.p. geometry<sup>16</sup> and in  $[\text{Co}(\text{AsMePh}_2\text{O})_4(\text{NO}_3)]$  of  $C_{4v}$  symmetry.<sup>21</sup>

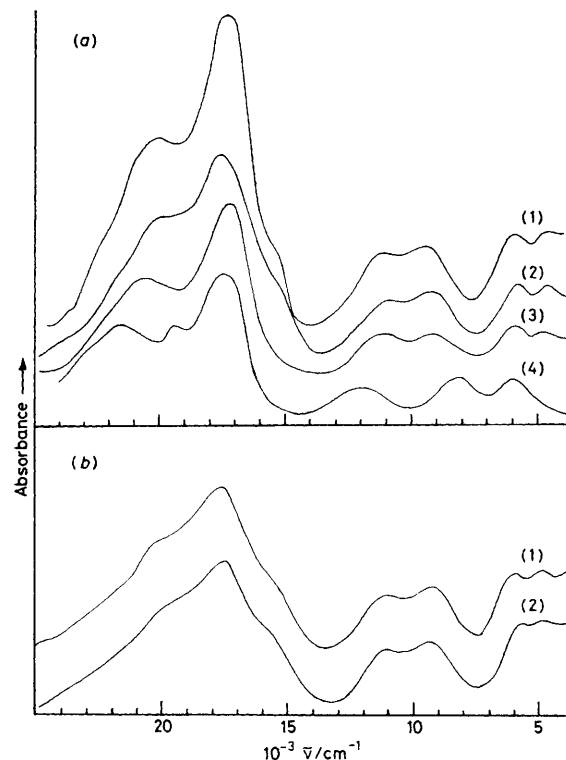


FIGURE 6 Electronic reflectance spectra of  $\text{Co}^{2+}$ -exchanged materials after heating at  $900^\circ\text{C}$ . (a)  $\alpha$  Forms:  $\text{Co}_{1.0}$  (1);  $\text{Co}_{0.73}$  (2);  $\text{Co}_{0.47}\text{Na}_{0.3}$  (3);  $\text{Co}_{0.33}\text{Na}_{0.5}$  (4). (b)  $\gamma$  Forms:  $\text{Co}_{0.58}$  (1);  $\text{Co}_{0.4}$  (2)

The spectra of these materials fit the energy-level diagrams for five-co-ordinate geometries not only as regards number and relative intensities of the bands, but also as regards the energies (assuming that the four bands in the near-i.r. region assigned to t.b.p. geometry arise from splitting of parent  ${}^4E''$  and  ${}^4E'$   $D_{3h}$  levels). Thus, for  $\text{Co}^{2+}$  in a regular t.b.p. field, transitions are expected at ( $Dq_{ax} = Dq_{base} = 900$ ;  $B = ca. 800\text{ cm}^{-1}$ ):  $ca. 4\,000$  ( ${}^4E''$ ),  $11\,300$  ( ${}^4E'$ ),  $16\,000$  ( ${}^4A_2'$ ), and  $19\,400\text{ cm}^{-1}$  ( ${}^4E''$ ) using literature energy-level diagrams.<sup>22</sup> For the s.p. case (and using the same crystal-field parameters) the transitions are expected at  $ca. 4\,800$  ( ${}^4B_2$ , electronically forbidden),  $7\,500$  ( ${}^4E$ ),  $12\,800$  ( ${}^4B_1$ ),  $17\,000$  ( ${}^4E$ ), and  $22\,000\text{ cm}^{-1}$  ( ${}^4A_2$ ). Given the various approximations made, these energies are in quite close agreement with those found experimentally [see Figure 6(a)].

On the same basis, the  $\text{Co}^{2+}$   $\gamma$  forms contain a t.b.p. site at both high and low loadings [Figure 6(b)].

Turning to the non-layer  $\text{Ni}^{2+}$ -containing materials, it appears that the degree of loading is now more important than differences in interplanar spacing, when compared to the case in anhydrous layer analogues. Both high- and low-loaded  $\gamma$  forms and high-loaded  $\alpha$  forms give spectra which, although not identical, are very similar to those which we assigned as arising from a distorted tetrahedral geometry.<sup>2</sup> However, at low loading the  $\alpha$  forms give a very different type of spectrum, with bands at  $5\,750$ ,  $7\,150$ ,  $12\,050$ ,  $20\,400$ , and  $22\,470\text{ cm}^{-1}$ ,

which clearly do not arise from either octahedral or tetrahedral geometries (see Figure 7). Following the same reasoning as outlined above, a five-co-ordinate geometry can be assigned. Indeed, the spectra are readily compared with those expected on the basis of trigonal-bipyra-

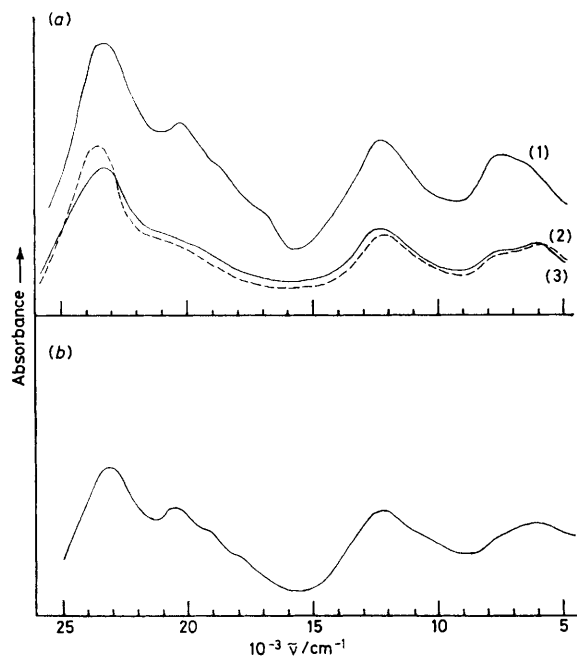


FIGURE 7 Electronic reflectance spectra of  $\text{Ni}^{2+}$ -exchanged materials after heating at  $900^\circ\text{C}$ . (a)  $\alpha$  Forms:  $\overline{\text{Ni}}_{0.66}$  (1);  $\overline{\text{Ni}}_{0.33}\overline{\text{Na}}_{0.34}$  (2);  $\overline{\text{Ni}}_{0.33}\overline{\text{Na}}_{0.44}$  (3). (b)  $\gamma$ - $\overline{\text{Ni}}_{0.2}$  (same spectra for loadings up to 100%)

midal geometry rather better than those of model complexes, most of which involve multidentate ligands imposing a tetrahedral distortion.<sup>23</sup> A tentative assignment is:  $5\,750$  and  $7\,250\text{ cm}^{-1}$ , components from  ${}^3E''$  in regular  $D_{3h}$  symmetry;  $12\,050\text{ cm}^{-1}$ , components from  ${}^3A_2'$  and  ${}^3A_1''$  levels (forbidden in pure  $D_{3h}$  symmetry);  $20\,400\text{ cm}^{-1}$ ,  ${}^3E''$  (symmetry forbidden); and  $22\,470\text{ cm}^{-1}$ ,  ${}^3A_2'$  (symmetry allowed, ground state  ${}^3E''$ ). A crude, but reasonable, fit to the literature diagrams<sup>24</sup> is given with  $Dq = ca. 920\text{ cm}^{-1}$ , suggesting that the geometry present is quite close to  $D_{3h}$ . The different stereochemistries present in lower-loaded  $\alpha$  layer forms heated at  $400^\circ\text{C}$  are now no longer present; the same t.b.p. geometry is now given for both  $\alpha$ - $\overline{\text{Ni}}_{0.33}\overline{\text{Na}}_{0.34}$  and  $\alpha$ - $\overline{\text{Ni}}_{0.33}\overline{\text{Na}}_{0.44}$  (see Figure 7).

**Copper(II)-containing materials.** With  $\text{Cu}^{2+}$ -loaded materials it is much more difficult to suggest changes in the geometry of the cavity in the absence of e.s.r. spectra<sup>25</sup> (as expected, given the high loading, all materials gave only broad exchanged signals at  $77\text{ K}$ ; these are not reported). As regards the room-temperature (r.t.) materials, the most one can say is that the tetragonal distortion decreases in the  $\gamma$  forms, the band maxima being at measurably lower energies than those in the  $\alpha$  forms (see Table 3).

The anhydrous (layered)  $\alpha$  forms give essentially

similar spectra as for the r.t. forms. However, in the  $\gamma$  form there is evidence for the building in of a geometry which is not tetragonal octahedral, as the loading decreases (see Figure 8). This second species gives a peak at  $ca. 8\,000\text{ cm}^{-1}$ , and the whole spectrum now extends from  $20\,000$  to  $ca. 5\,000\text{ cm}^{-1}$ . The only comparison with literature data which appears reasonable is with the spectrum of  $\text{Cu}^{2+}$ - $\gamma$ - $\text{Al}_2\text{O}_3$ , in which the broadening is due to the simultaneous presence of both tetragonal octahedral and (close to) tetrahedral geometries.<sup>26</sup> We suggest that a slightly more flattened geometry is present in our case.<sup>27</sup> Below  $50\%$  loading, inhomogeneous materials were obtained, which may be connected with the presence of this second species.

After heating at  $950^\circ\text{C}$ , the  $\alpha$  forms gave a well defined band with a peak at  $11\,500\text{ cm}^{-1}$  and a shoulder at  $ca. 9\,200\text{ cm}^{-1}$ . Although there appear to be no examples of

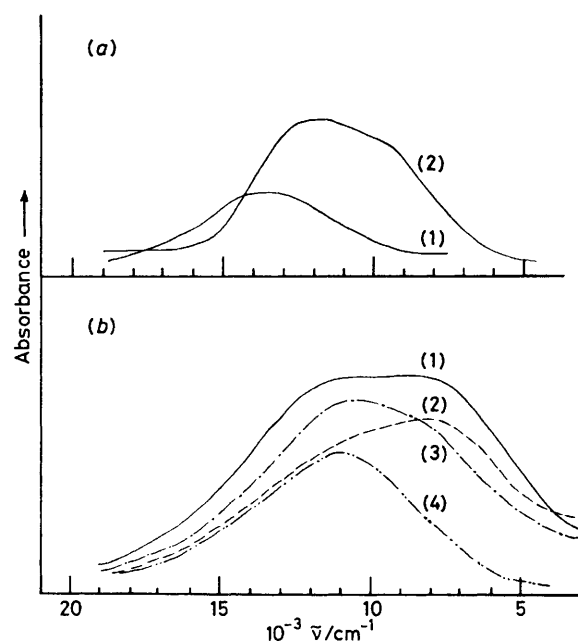


FIGURE 8 Electronic reflectance spectra of  $\text{Cu}^{2+}$ -containing materials. (a)  $\alpha$  Forms:  $\overline{\text{Cu}}_{0.5}\overline{\text{H}}_{0.66}\overline{\text{Na}}_{0.33}\cdot 3\overline{\text{H}}_2\text{O}$  (similar spectra for loadings  $\geq 50\%$ ) (1);  $\overline{\text{Cu}}_{0.33}\overline{\text{Na}}_{0.44}$  (after heating at  $900^\circ\text{C}$ ) (2). (b)  $\gamma$  Forms after heating at  $400^\circ\text{C}$ :  $\overline{\text{Cu}}_{0.84}$  (1);  $\overline{\text{Cu}}_{0.7}$  (2);  $\overline{\text{Cu}}_{1.0}$  (3);  $\overline{\text{Cu}}_{0.24}$  (4)

$\text{CuO}_5$  chromophores in the literature to allow comparisons to be made, this change in spectrum would be in agreement with a five-co-ordinate geometry being present (a choice between t.b.p. and s.p. cannot be made in the absence of e.s.r. spectra).<sup>25</sup> Degree of loading again appears to be important; at low loading the spectrum changes, for both acetate- or nitrate-prepared materials. The major broad band lies at  $ca. 11\,250\text{ cm}^{-1}$ , but there is evidence for a shoulder to higher energy, at  $ca. 15\,500\text{ cm}^{-1}$  (see Table 3). This may indicate that a more highly tetragonally distorted  $\text{CuO}_4 + 2\text{O}$  system is present.<sup>28</sup>

**Conclusions.**—There have been many spectroscopic studies of zeolites exchanged with transition-metal ions over the past 10 years. However, it is only very



recently that evidence has been accumulated to show that variable geometries can be obtained during the solvation, evacuation, and activation treatments. Thus, co-ordination number changes from six to four to five are believed to occur in cobalt-exchanged NaA zeolites<sup>29</sup> and this is supported by more recent results.<sup>30</sup> In addition, e.s.r. spectra of low-loaded copper(II) A and Y zeolites also indicate that five-co-ordinate species are present<sup>31,32</sup> and evidence has been presented for near-neighbour interactions in Ce<sup>3+</sup>-Cu<sup>2+</sup>-exchanged Y zeolites.<sup>33</sup>

The evidence presented here shows that there is similar stereochemical variability in layered-structure materials. Indeed, the spectroscopic evidence for co-ordination number changes from six to four to five is particularly good for Co<sup>2+</sup> and Ni<sup>2+</sup> and it is clear that the other phases necessarily present in partially exchanged materials can cause drastic changes in co-ordination geometry (the evidence for Cu<sup>2+</sup> is much less clear). The implications of these results for the catalytic properties of the materials are being investigated. Direct bond-distance information and support for the co-ordination numbers suggested are being sought from extended X-ray absorption fine structure (e.x.a.f.s.) spectroscopy and will be reported shortly.

[0/1903 Received, 9th December, 1980]

#### REFERENCES

- S. Allulli, C. Ferragina, A. La Ginestra, M. A. Massucci, and N. Tomassini, *J. Chem. Soc., Dalton Trans.*, 1977, 1879.
- S. Allulli, C. Ferragina, A. La Ginestra, M. A. Massucci, N. Tomassini, and A. A. G. Tomlinson, *J. Chem. Soc., Dalton Trans.*, 1976, 2115.
- 'Zeolite Chemistry and Catalysis,' ed. J. A. Rabo, American Chemical Society Monograph, 1976, vol. 191.
- C. Ferragina, A. La Ginestra, M. A. Massucci, N. Tomassini, and A. A. G. Tomlinson, 5th International Conference on Thermal Analysis, Kyoto, August 1977; Proceedings, p. 424.
- Y. Onoue, Y. Mizutani, S. Akiyama, Y. Izumi, and Y. Watanabe, *Chemtech.*, 1977, 36.
- D. N. Bernart and A. R. Wreath, *Anal. Chem.*, 1955, **27**, 400.
- A. Clearfield, R. H. Blessing, and J. A. Stynes, *J. Inorg. Nucl. Chem.*, 1968, **30**, 2249.
- A. La Ginestra and M. A. Massucci, *Thermochim. Acta*, 1979, **32**, 241.
- C. K. Jorgensen, 'Absorption Spectra and Chemical Bonding in Complexes,' Pergamon, London, 1962.
- A. Clearfield and G. D. Smith, *Inorg. Chem.*, 1969, **8**, 431.
- S. Yamanaka and M. Tanaka, *J. Inorg. Nucl. Chem.*, 1979, **41**, 45.
- E. König, *Struct. Bonding (Berlin)*, 1971, **9**, 175.
- L. Sacconi, *Transition Met. Chem.*, 1968, **4**, 199.
- See for example, R. Stomberg, I-B. Svensson, and A. A. G. Tomlinson, *Acta Chem. Scand.*, 1973, **27**, 1192.
- C. Furlani, *Coord. Chem. Rev.*, 1968, **3**, 141.
- D. F. Averill, J. I. Legg, and D. L. Smith, *Inorg. Chem.*, 1972, **11**, 2344.
- J. Lewis, R. S. Nyholm, and G. A. Rodley, *Nature (London)*, 1965, **207**, 12; M. Gerloch, J. Kohl, J. Lewis, and W. Urland, *J. Chem. Soc. A*, 1970, 3269.
- F. Pepe, M. Schiavello, and G. Ferraris, *J. Solid State Chem.*, 1975, **12**, 63.
- A. C. Villa, C. Guastini, P. Porta, and A. A. G. Tomlinson, *J. Chem. Soc., Dalton Trans.*, 1978, 956; C. Bellitto, A. A. G. Tomlinson, C. Furlani, and G. De Munno, *Inorg. Chim. Acta*, 1978, **27**, 269.
- W. Byers, A. B. P. Lever, and R. V. Parish, *Inorg. Chem.*, 1968, **7**, 1835; B. A. Coyle and J. A. Ibers, *ibid.*, 1970, **9**, 767.
- M. Gerloch, J. Kohl, J. Lewis, and W. Urland, *J. Chem. Soc. A*, 1970, 3283.
- M. Ciampolini, *Struct. Bonding (Berlin)*, 1969, **6**, 52, and refs. therein.
- L. Sacconi, *Coord. Chem. Rev.*, 1972, **8**, 351.
- M. Ciampolini, *Inorg. Chem.*, 1966, **5**, 35.
- B. J. Hathaway and A. A. G. Tomlinson, *Coord. Chem. Rev.*, 1970, **5**, 1; B. J. Hathaway and D. E. Billing, *ibid.*, p. 143.
- J. J. Freeman and R. M. Friedman, *J. Chem. Soc., Faraday Trans. 1*, 1977, 758.
- A. Yokoi and W. A. Addison, *Inorg. Chem.*, 1977, **16**, 1341; J. R. Wasson, M. W. Richardson, and W. E. Hatfield, *Z. Naturforsch., Teil B*, 1978, **32**, 557.
- D. E. Billing, B. J. Hathaway, and P. Nicholls, *J. Chem. Soc. A*, 1969, 316.
- S. Akbar and R. W. Joyner, *J. Chem. Soc., Chem. Commun.*, 1978, 548.
- H. Praleau and G. Condourier, *J. Chem. Soc., Faraday Trans. 1*, 1979, 2601.
- R. G. Heman, *Inorg. Chem.*, 1979, **18**, 995.
- J. C. Conesa and J. Soria, *J. Chem. Soc., Faraday Trans. 1*, 1979, 406.
- J. C. Conesa and J. Soria, *J. Chem. Soc., Faraday Trans. 1*, 1979, 423.